Journal of Physics A: Mathematical and Theoretical

**PAPER**

# Higher-order rogue wave solutions of the Sasa–Satsuma equation

**IOP** Publishing Journal of Physics A: Mathematical and Theoretical

J. Phys. A: Math. Theor. **55** (2022) 235701 (24pp) https://doi.org/10.1088/1751-8121/ac6917

# Higher-order rogue wave solutions of the Sasa–Satsuma equation

**Bao-Feng Feng**[1], **Changyan Shi**[2], **Guangxiong Zhang**[2] **and Chengfa Wu**[2,*]

[1] School of Mathematical and Statistical Sciences, The University of Texas Rio Grande Valley Edinburg, Edinburg, TX 78541-2999, United States of America

[2] Institute for Advanced Study, Shenzhen University, Shenzhen 518060, People's Republic of China

E-mail: cfwu@szu.edu.cn

Received 15 February 2022, revised 12 April 2022
Accepted for publication 21 April 2022
Published 16 May 2022

**Abstract**

Up to the third-order rogue wave solutions of the Sasa–Satsuma (SS) equation are derived based on the Hirota's bilinear method and Kadomtsev–Petviashvili hierarchy reduction method. They are expressed explicitly by rational functions with both the numerator and denominator being the determinants of even order. Four types of intrinsic structures are recognized according to the number of zero-amplitude points. The first- and second-order rogue wave solutions agree with the solutions obtained so far by the Darboux transformation. In spite of the very complicated solution form compared with the ones of many other integrable equations, the third-order rogue waves exhibit two configurations: either a triangle or a distorted pentagon. Both the types and configurations of the third-order rogue waves are determined by different choices of free parameters. As the nonlinear Schrödinger equation is a limiting case of the SS equation, it is shown that the degeneration of the first-order rogue wave of the SS equation converges to the Peregrine soliton.

Keywords: Sasa–Satsuma equation, rogue wave, Kadomtsev–Petviashvili hierarchy reduction method

(Some figures may appear in colour only in the online journal)

*Author to whom any correspondence should be addressed.

## 1. Introduction

The study of the nonlinear Schrödinger (NLS) equation lies at the forefront of applied mathematics and mathematical physics since it has been recognized as a generic model for describing the evolution of slowly varying wave packets in general nonlinear wave system [1, 2]. It arises in a variety of physical contexts such as nonlinear optics [3–5], Bose–Einstein condensates [6], water waves [7] and plasma physics [8].

In the context of nonlinear optics, when the width of optical pulses is less than 1 ps, higher-order nonlinear effects have to be taken into account and the NLS equation should be modified. As a result, a generalized NLS (gNLS) equation [4]

$$\mathrm{i}q_z + \frac{1}{2}q_{\tau\tau} + |q|^2 q + \mathrm{i}\epsilon(\beta_1 q_{\tau\tau\tau} + \beta_2|q|^2 q_\tau + \beta_3 q(|q|^2)_\tau) = 0, \quad (1)$$

is derived, where $\beta_1$, $\beta_2$ and $\beta_3$ are the parameters related to the third-order dispersion, self-steepening and stimulated Raman scattering, respectively. Due to the complexity of the gNLS equation, the study is mainly numerical. However, in some special cases, the gNLS equation becomes integrable and is available for rigorous analysis. For example, when $\beta_1 : \beta_2 : \beta_3 = 1 : 6 : 3$, it is an integrable equation called the Sasa–Satsuma (SS) equation [9, 10]. Under this case, a gauge transformation

$$\begin{cases} u(x,t) = q(\tau, z)\exp\left\{\dfrac{-\mathrm{i}}{6\varepsilon}\left(\tau - \dfrac{z}{18\varepsilon}\right)\right\}, \\ t = z, \\ x = \tau - \dfrac{z}{12\varepsilon}, \end{cases} \quad (2)$$

brings the SS equation into the form

$$u_t + \varepsilon(u_{xxx} + 6|u|^2 u_x + 3u(|u|^2)_x) = 0. \quad (3)$$

It is noted that when $\beta_1 : \beta_2 : \beta_3 = 1 : 6 : 0$, equation (1) is also an integrable equation called Hirota equation [11].

Rogue waves, which are initially used for the description of the spontaneous and monstrous ocean surface waves, have attracted much attention in the past two decades [12–14]. With the experimental developments, extensive theoretical studies have also been focused on rogue waves [15–18]. The mathematical study of rogue waves originated from a rational solution of the NLS equation, which is called the Peregrine soliton [19]. Since the higher-order rogue waves were discovered by Akhmediev *et al* [20], significant progress on the study of higher-order rogue waves has been achieved including the multi-component generalizations of some integrable equations [21–25]. Based on the Riemann–Hilbert approach [26], rogue waves of infinite order have been revealed [27]. In addition, rogue waves on the periodic background [28–31] have been comprehensively investigated. Very recently, Yang and Yang [32, 33] performed an in-depth study on the universal wave patterns of many integrable equations by connecting the explicit expressions of rogue waves with the Yablonskii–Vorob'ev polynomial hierarchy. There are several methods available in constructing rogue wave solutions such as the Darboux transformation [34, 35] and Hirota's bilinear method [36, 37]. These methods seem quite different, however, they have the same spirit to take the limit of breather solutions in which the spectral parameter tends to the branch point of the spectrum [38]. In bilinear method [37], the action of differential operators on kernel function is equivalent to the limiting process in Darboux transformation. The wave number in the kernel function is basically the spectral parameter in Lax pair.

In addition to the NLS equation, Hirota's bilinear method has been applied to find general rogue wave solutions for a variety of integrable equations such as the Ablowitz–Ladik equation [39], the Davey–Stewartson I and II equations [40, 41], the Yajima–Oikawa equation [42, 43], a long-wave-short-wave model of Newell type [44], the derivative NLS equation [45], the three-wave equation [46], the Boussinesq equation [47] and the coupled NLS equation (Manakov system) [33]. In this method, we start with a scalar function which we call the kernel function. Then, we construct a determinant called tau function with differential operators acting on the kernel function. Under some dispersion relations, it can be shown that the tau function satisfies a set of bilinear equations. Next, through a series of reductions including dimension reduction and complex conjugate reduction, we reduce the set of bilinear equations to the bilinear form of the underlying soliton equation. Finally, we can express the general rogue wave solutions in terms of the tau functions satisfying reduction conditions. We remark here that the dimension reduction is crucial among all the reductions.

In this paper, we attempt to study the rogue wave solutions of the SS equation

$$u_t = u_{xxx} - 6c|u|^2 u_x - 3cu\left(|u|^2\right)_x, \tag{4}$$

by Hirota's bilinear method, where $c$ is a real constant. Despite extensive efforts on the derivation of rogue waves, the higher-order rogue wave solutions of the SS equation have not been reported before. As far as we know, only the first- and second-order rogue wave solutions [35, 48–50] of the SS equation have been constructed in explicit forms. Intriguingly, as shown in [48], the first-order rogue waves of the SS equation demonstrate a distinctive feature, which is the so-called twisted-rogue wave (TRW) pair (see figure 2).

In Sato theory developed by Kyoto school in 1980s, the original Kadomtsev–Petviashvili hierarchy is named Kadomtsev–Petviashvili hierarchy of A-type or AKP hierarchy according to the classification of Lie algebra, then its sub-hierarchies of B-type, C-type and D-type are called BKP, CKP and DKP hierarchies, respectively [51]. It is known that the NLS equation belongs to the AKP hierarchy while the SS equation belongs to the CKP hierarchy. In order to construct rogue wave solutions of the SS equation, we have to start with a kernel function of $2 \times 2$ matrix and a determinant of even order with differential operators acting on the matrix kernel function. Therefore, as explained in subsequent sections, the reduction procedure and the rogue wave solutions are much more complicated. To be specific, the tau functions associated with the first-, second- and third-order rogue wave solutions are determinants of $2 \times 2$, $4 \times 4$ and $6 \times 6$, respectively.

The remainder of this paper is organized as follows. In section 2, the procedure in deriving rogue wave solutions of the SS equation (4) by applying Hirota's bilinear method and Kadomtsev–Petviashvili hierarchy reduction technique is outlined. Then we present the explicit expression of first-order rogue waves of the SS equation and analyze their dynamics in section 3. In addition, the degeneration of the first-order rogue wave to the Peregrine soliton is discussed as well. In sections 4 and 5, we provide the explicit expressions of second- and third-order rogue waves of the SS equation respectively. In particular, the third-order solutions are expressed in terms of $6 \times 6$ determinants, where the associated $\tau$-functions are polynomials of degree 24 in $x$ and $t$, and to the best of our knowledge, this is the first time that the third-order rogue waves are provided in explicit form. Finally, we summarize the main results of this paper in section 6.

## 2. Outline of the derivation for rogue waves

In this section, we use Hirota's bilinear method to derive the rogue wave solutions of the SS equation (4) based on the KP reduction technique. The main idea is given briefly below. Similar to the cases of dark soliton and breather solutions [52, 53], the SS equation (4) is transformed into a set of three bilinear equations (see proposition 3.1 in [52])

$$\begin{aligned}
&\left(D_x^2-4c\right) f\cdot f=-4cgg^*\\
&\left(D_x^3-D_t+3\mathrm{i}\kappa D_x^2-3\left(\kappa^2+4c\right)D_x-6\mathrm{i}\kappa c\right) g\cdot f+6\mathrm{i}\kappa cqg=0,\\
&\left(D_x+2\mathrm{i}\kappa\right) g\cdot g^*=2\mathrm{i}\kappa qf
\end{aligned} \tag{5}$$

under the non-zero boundary condition at $\pm\infty$ by the variable transformation

$$u=\frac{g}{f}\mathrm{e}^{\mathrm{i}\left(\kappa(x-6ct)-\kappa^3 t\right)}, \tag{6}$$

where $\kappa$ is real, $f$ is a real-valued function, $g$ is a complex-valued function, $q$ is an auxiliary tau function and $D$ is the Hirota's bilinear operator [36] defined by

$$D_x^m D_t^n f\cdot g=\left(\frac{\partial}{\partial x}-\frac{\partial}{\partial x'}\right)^m\left(\frac{\partial}{\partial t}-\frac{\partial}{\partial t'}\right)^n[f(x,t)g(x',t')]\bigg|_{x'=x,t'=t}. \tag{7}$$

We start with a specially designed tau function of the extended KP hierarchy that has two discrete indices $k$ and $l$. We introduce a kernel, which is a $2\times 2$ matrix

$$M^{kl}=\begin{pmatrix} m_{11}^{kl} & m_{12}^{kl}\\ m_{21}^{kl} & m_{22}^{kl}\end{pmatrix}, \tag{8}$$

with entries

$$m_{\alpha\beta}^{kl}=\frac{1}{p_\alpha+q_\beta}\left(-\frac{p_\alpha-a}{q_\beta+a}\right)^k\left(-\frac{p_\alpha-b}{q_\beta+b}\right)^l e^{\xi_\alpha+\eta_\beta}, \tag{9}$$

$$\xi_\alpha=p_\alpha x+p_\alpha^2 y+p_\alpha^3 t+\frac{1}{p_\alpha-a}r+\frac{1}{p_\alpha-b}s+\xi_{\alpha 0}, \tag{10}$$

$$\eta_\beta=q_\beta x-q_\beta^2 y+q_\beta^3 t+\frac{1}{q_\beta+a}r+\frac{1}{q_\beta+b}s+\eta_{\beta 0}, \tag{11}$$

for $1\leqslant\alpha,\beta\leqslant 2$, where $p_\alpha, q_\beta, \xi_{\alpha 0}, \eta_{\beta 0}, a, b$ are complex constants. Let $A_i$ and $B_j$ be differential operators of order $i$ and $j$, respectively, defined by

$$A_i(p)=\sum_{n=0}^{i}\frac{a_{i-n}(p)}{n!}(p\partial_p)^n,\qquad B_j(q)=\sum_{n=0}^{j}\frac{b_{j-n}(q)}{n!}(q\partial_q)^n, \tag{12}$$

where $a_k(p)$ $(1\leqslant k\leqslant i)$ and $b_l(q)$ $(1\leqslant l\leqslant j)$ are complex constants. Then, we define a $2N\times 2N$ determinant

$$\tau_{kl}=\det\left(M_{i_\nu j_\mu}^{kl}\right)_{1\leqslant\nu,\mu\leqslant N}, \tag{13}$$

where $M^{kl}_{i_\nu j_\mu}$ is a $2\times 2$ matrix defined by

$$M^{kl}_{i_\nu j_\mu}=\begin{pmatrix}A_{i_\nu}(p_1)B_{j_\mu}(q_1)m^{kl}_{11} & A_{i_\nu}(p_1)B_{j_\mu}(q_2)m^{kl}_{12}\\ A_{i_\nu}(p_2)B_{j_\mu}(q_1)m^{kl}_{21} & A_{i_\nu}(p_2)B_{j_\mu}(q_2)m^{kl}_{22}\end{pmatrix}, \tag{14}$$

and $(i_1,i_2,\ldots,i_N)$, $(j_1,j_2,\ldots,j_N)$ are arbitrary sequence of indices. A remarkable property of the function $\tau_{kl}$ is that it satisfies eleven bilinear equations (the details are provided in appendix A).

Next, we perform a type C-reduction by requiring

$$q_j=p_j,\qquad b=-a,\qquad \xi_{j0}=\eta_{j0}, \tag{15}$$

and a dimension reduction by requiring

$$\left(\partial_r+\partial_s-\frac{1}{c}\partial_x\right)\tau_{kl}=C\tau_{kl}, \tag{16}$$

where $C$ is a constant. By doing so, one obtains the following bilinear equations

$$\left(D_x^2-4c\right)\tau_{kl}\cdot\tau_{kl}=-2c\left(\tau_{k+1,l}\tau_{k-1,l}+\tau_{k,l+1}\tau_{k,l-1}\right), \tag{17}$$

$$\left(D_x^3-D_t+3aD_x^2+3\left(a^2-2c\right)D_x-6ac\right)\tau_{k+1,l}\cdot\tau_{kl}+6ac\tau_{k+1,l+1}\tau_{k,l-1}=0, \tag{18}$$

$$\left(D_x^3-D_t-3aD_x^2+3\left(a^2-2c\right)D_x+6ac\right)\tau_{k,l+1}\cdot\tau_{kl}-6ac\tau_{k+1,l+1}\tau_{k-1,l}=0, \tag{19}$$

$$(D_x+2a)\tau_{k+1,l}\cdot\tau_{k,l+1}=2a\tau_{k+1,l+1}\tau_{kl}. \tag{20}$$

Thirdly, we can realize the complex conjugate condition

$$\tau^*_{k0}=\tau_{0k},\quad \tau^*_{kk}=\tau_{kk}, \tag{21}$$

by requiring

$$p_1=p_2^*,\qquad \xi_{10}=\xi^*_{20}. \tag{22}$$

Notice that the C-reduction also implies that

$$\tau_{kl}=\tau_{-l,-k}. \tag{23}$$

Thus, if we define

$$\begin{aligned}&f(x,t)=\tau_{00}(x-6ct,t),\\&q(x,t)=\tau_{11}(x-6ct,t),\\&g(x,t)=\tau_{10}(x-6ct,t)=\tau_{0,-1}(x-6ct,t),\end{aligned} \tag{24}$$

then according to the complex conjugate condition, we have

$$g^*(x,t)=\tau_{-1,0}(x-6ct,t)=\tau_{01}(x-6ct,t). \tag{25}$$

Consequently, by taking $k=l=0$ and $a=\mathrm{i}\kappa$, the bilinear equations (17), (18) and (20) are reduced to exactly (5) while (19) is merely the complex conjugate of (18).

It is commented here the key point in deriving the rogue wave solutions to the SS equation is to realize the dimension reduction (16).

## 3. First-order rogue wave

In this section, we present the first-order rogue wave of the SS equation (4)

$$u = \frac{g}{f} e^{i\left(\kappa(x-6ct)-\kappa^3 t\right)}, \tag{26}$$

where

$$f(x,t) = \tau_{00}(x-6ct,t), \qquad g(x,t) = \tau_{10}(x-6ct,t), \tag{27}$$

and $\tau_{kl}$ is defined as

$$\tau_{kl} = |M_{11}|_{\substack{p_1=q_1=\xi \\ p_2=q_2=\xi^*}}, \tag{28}$$

with

$$A_1(p) = a_0^{(0)}(p\partial_p) + a_1^{(0)}, \qquad B_1(q) = b_0^{(0)}(q\partial_q) + b_1^{(0)}, \tag{29}$$

$\xi$ and $\xi^*$ being a pair of complex conjugate roots of the quartic equation

$$\frac{1}{(p-i\kappa)^2} + \frac{1}{(p+i\kappa)^2} + \frac{1}{c} = 0. \tag{30}$$

Here, the parameters $p_j, q_j, \xi_{j0}, \eta_{j0}, a_n^{(0)}, b_n^{(0)}, (j=1,2, n=0,1)$ satisfy the constraints

$$\begin{aligned} &p_j = q_j, \quad p_j = p_{3-j}^*, \quad \xi_{j0} = \eta_{j0}, \quad \xi_{j0} = \xi_{3-j,0}^*, \\ &a_n^{(0)} = b_n^{(0)}, \quad a_n^{(0)}(p_j) = [a_n^{(0)}(p_{3-j})]^*, \end{aligned} \tag{31}$$

where $*$ denotes complex conjugation. Let us provide a brief proof. First, we introduce a notion

$$\widetilde{D}_{r,s,x} = \partial_r + \partial_s - \frac{1}{c}\partial_x, \tag{32}$$

then since

$$\widetilde{D}_{r,s,x} e^{\xi_i} = \left(\frac{1}{p_i - a} + \frac{1}{p_i + a} - \frac{p_i}{c}\right) e^{\xi_i}, \tag{33}$$

$$\widetilde{D}_{r,s,x} e^{\eta_j} = \left(\frac{1}{q_j - a} + \frac{1}{q_j + a} - \frac{q_j}{c}\right) e^{\eta_j}, \tag{34}$$

we define

$$F(p) = \frac{1}{p-a} + \frac{1}{p+a} - \frac{p}{c}, \qquad F_m(p) = (p\partial_p)^m F(p), \tag{35}$$

and denote a pair of complex conjugate roots for

$$F_1(p) = -\frac{p}{(p-a)^2} - \frac{p}{(p+a)^2} - \frac{p}{c}, \tag{36}$$

with $a = i\kappa$, which is equivalent to (30), by $\xi$ and $\xi^*$. Since

$$\widetilde{D}_{r,s,x}A_1(p_\alpha)B_1(q_\beta)m^{kl}_{\alpha\beta}\Big|_{\substack{p_1=q_1=\xi\\ p_2=q_2=\xi^*}} = \left[F(p_\alpha)+F(q_\beta)\right]A_1(p_\alpha)B_1(q_\beta)m^{kl}_{\alpha\beta}\Big|_{\substack{p_1=q_1=\xi\\ p_2=q_2=\xi^*}}, \tag{37}$$

where $\alpha, \beta = 1, 2$, it then follows

$$\widetilde{D}_{r,s,x}|M_{11}|_{\substack{p_1=q_1=\xi\\ p_2=q_2=\xi^*}} = 2[F(\xi)+F(\xi^*)]|M_{11}|_{\substack{p_1=q_1=\xi\\ p_2=q_2=\xi^*}}, \tag{38}$$

which realizes the dimension reduction. Thus, the first-order rogue wave solution is approved.

We note that the algebraic equation (30) can be rewritten as

$$p^4 + 2\left(c+\kappa^2\right)p^2 + \kappa^2(\kappa^2-2c) = 0. \tag{39}$$

When $c\left(c+4\kappa^2\right) < 0$, equation (39) has at least one pair of complex conjugate roots with nonzero real part and nonzero imaginary part. Hence, the rogue wave solution (26) exists if and only if $c$ and $\kappa$ satisfy the conditions

$$c < 0, \qquad c + 4\kappa^2 > 0. \tag{40}$$

On the other hand, as (39) is a quartic equation in $\xi$, it has four roots (counting multiplicity). Due to the fact that all coefficients of (39) are real, these roots demonstrate a symmetric structure, that is, if $\xi$ is a root of (39), then the other three roots are $-\xi$ and $\pm\xi^*$. As a result, they can be explicitly expressed as

$$\pm\frac{1}{\sqrt{2}}\left[\left(|\kappa|(\kappa^2-2c)^{1/2}-c-\kappa^2\right)^{1/2} \pm i\left(|\kappa|(\kappa^2-2c)^{1/2}+c+\kappa^2\right)^{1/2}\right]. \tag{41}$$

Specifically, the tau functions related to the first-order rogue wave can be simplified into the form

$$\begin{aligned} f(x,t) &= \left|A_{11}\left(\chi_{11}^2+\Delta_{11}\right)\right|^2 - A_{12}^2(\chi_{12}\chi_{21}+\Delta_{12})^2,\\ g(x,t) &= B_{11}B_{22}[(\chi_{11}-C_1)(\chi_{11}-D_1)+\Delta_{11}]\\ &\quad\times[(\chi_{22}-C_2)(\chi_{22}-D_2)+\Delta_{22}] - B_{12}B_{21}\left[(\chi_{12}-C_1)(\chi_{21}-D_2)\right.\\ &\quad\left.+\Delta_{12}\right][(\chi_{21}-C_2)(\chi_{12}-D_1)+\Delta_{21}], \end{aligned} \tag{42}$$

where $(1 \leqslant i, j \leqslant 2)$

$$\begin{aligned} &\chi_{ij} = x - 6ct + 3p_i^2 t + \theta_{ij}, && \Delta_{ij} = \frac{1}{(p_i+p_j)^2}, && A_{ij} = \frac{1}{p_i+p_j},\\ &B_{ij} = A_{ij}\frac{a-p_i}{a+p_j}, && C_i = \frac{1}{a-p_i}, && D_j = \frac{1}{a+p_j},\\ &\theta_{ij} = -\frac{1}{p_i+p_j} + \frac{a_1^{(0)}(p_i)}{a_0^{(0)}(p_i)}\frac{1}{p_i}. \end{aligned} \tag{43}$$

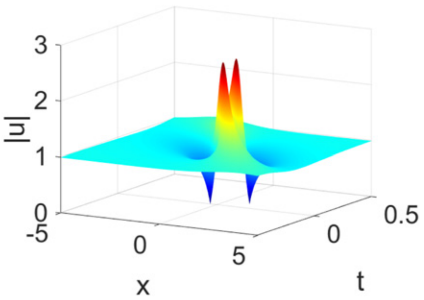


**Figure 1.** The first-order rouge wave solution with parameter values $a = \sqrt{2}\mathrm{i}/\sqrt[4]{3}$, $c = -2/\sqrt{3}$, $a_0^{(0)} = 1$, $a_1^{(0)} = 0$.

We note that both of $f$ and $g$ are polynomials of degree 4 in $x$ and $t$, which are more complicated than the first-order rogue wave solutions of the NLS equation where the corresponding tau functions are polynomials of degree 2 in $x$ and $t$. For simplicity, we set

$$a_0^{(0)} = b_0^{(0)} = 1, \qquad a_1^{(0)} = b_1^{(0)} = 0. \tag{44}$$

In particular, if we take

$$a = \sqrt{2}\mathrm{i}/\sqrt[4]{3}, \qquad c = -2/\sqrt{3}, \qquad p_1 = q_1 = 1 + \mathrm{i}, \qquad p_2 = q_2 = 1 - \mathrm{i}, \tag{45}$$

then we can obtain a particular solution which is plotted in figure 1

$$u(x,t) = H\left(1 + \frac{G + \mathrm{i}F}{E}\right), \tag{46}$$

where

$$\begin{aligned}
H &= \frac{-\mathrm{i}3^{3/4}\sqrt{2} + \sqrt{3} - 3}{3^{3/4}\mathrm{i}\sqrt{2} + \sqrt{3} - 3} e^{\frac{\mathrm{i}\sqrt{2}\left(10t+\sqrt{3}x\right)}{3^{3/4}}}, \\
G &= 2\left(144\sqrt{3}t^2 + 144tx + 12\sqrt{3}x^2 + 12\left(\sqrt{3} - 9\right)t + \left(6 - 18\sqrt{3}\right)x + 7\sqrt{3}\right), \\
F &= \sqrt{2}\sqrt[4]{3}\left(2688\sqrt{3}t^3 - 16x^3 - 144\left(3\sqrt{3} - 3\right)t^2 - 4\left(\sqrt{3} - 9\right)x^2\right. \\
&\quad - 576t^2x - 96\sqrt{3}tx^2 - 8\left(6 - 18\sqrt{3}\right)tx - 8\left(5\left(\sqrt{3} - 3\right)\right)t \\
&\quad \left. + 4\left(3\sqrt{3} - 7\right)x - 7\sqrt{3} + 7\right), \\
E &= -2\left(16x^4 + 112\,896t^4 + 5760t^2x^2 + 21\,504\sqrt{3}t^3x + 256\sqrt{3}tx^3 - 48x^3\right. \\
&\quad - 2688\left(6\sqrt{3} + 3\right)t^3 - \left(768\sqrt{3} + 8640\right)t^2x - \left(576\sqrt{3} + 96\right)tx^2 + 56x^2 \\
&\quad \left. + \left(384\sqrt{3} + 3552\right)t^2 + \left(448\sqrt{3} + 96\right)tx - \left(112\sqrt{3} + 24\right)t - 28x + 7\right).
\end{aligned} \tag{47}$$

It can be seen that, compared with previous studies on first-order rogue wave solutions of the SS equation [35, 48, 54, 55], the solution obtained here is presented in a more compact form.

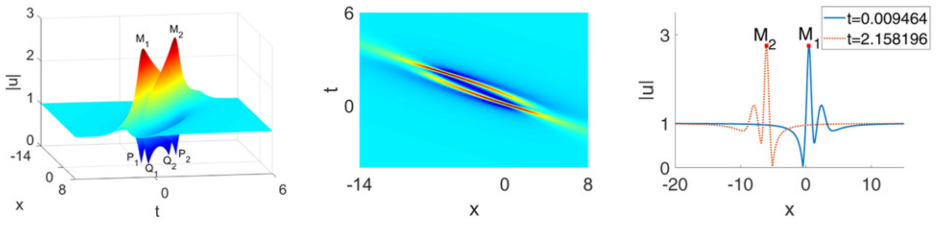


**Figure 2.** The TRW pair with parameter values $a = 0.45\mathrm{i}, c = -0.5, a_0^{(0)} = 1, a_1^{(0)} = 0$. (b) is the corresponding density plot and (c) corresponds to the time evolution of (a).

If we select another set of parameters

$$c = -\frac{1}{2}, \qquad a = \frac{9}{20}\mathrm{i}, \qquad p_1 = q_1 = \alpha + \mathrm{i}\beta, \qquad p_2 = q_2 = \alpha - \mathrm{i}\beta, \tag{48}$$

where

$$\begin{aligned} \alpha &= \frac{3}{20}\sqrt[4]{481}\sqrt{\frac{1}{2} + \frac{119}{18\sqrt{481}}}, \\ \beta &= \frac{3}{20}\sqrt[4]{481}\sqrt{\frac{1}{2} - \frac{119}{18\sqrt{481}}}, \end{aligned} \tag{49}$$

then we may express the corresponding solution in the same form as (46). As depicted in figure 2, this solution demonstrates a structure called TRW pair which was first reported in [48] and is a distinctive characteristic of the SS equation in contrast with many other integrable equations. It bears the name TRW pair due to the feature that it comprises two extended rogue-wave components bending toward each other and displaying an identical but antisymmetric structure. Further analysis indicates that this TRW pair possesses four zero-amplitude points $P_1, P_2, Q_1, Q_2$, which are located at $(-0.540\,049, 0.026\,462)$, $(-5.033\,412, 2.141\,300)$, $(-0.230\,825, 0.363\,748)$ and $(-5.342\,638, 1.804\,014)$ respectively, and has the maximum amplitude 2.758 536, which is attained at the points $M_1$ and $M_2$ that are located at $(0.471\,911, 0.009\,464)$ and $(-6.044\,867, 2.158\,196)$ respectively.

Interestingly, by tuning the values of the free parameter $a = \mathrm{i}\kappa$, the first-order rogue wave solutions display four types of intrinsic structures. To illustrate this, we set $c = -1/2$. The wave profiles are shown in figure 3 at three values of $a = 0.5\mathrm{i}$, $1.04\mathrm{i}$ and $1.84\mathrm{i}$ respectively. Specifically, starting from the TRW pair depicted in figure 2 ($a = 0.45\mathrm{i}$), the two zero-amplitude points $Q_1, Q_2$ first move toward each other and then merge into the same point $Q$ as $\kappa$ increases, whereas the other two zero-amplitude points $P_1, P_2$ remain, thereby giving rise to a rogue wave solution with three zero-amplitude points (see figures 3(a) and (d)). Furthermore, increasing $\kappa$ will cause the zero-amplitude point $Q$ disappears but remains to be a local minimum before becoming a saddle point (see figures 3(b) and (e)). Afterward, the rogue wave solution exhibits a relatively simpler structure, which consists of two different types. Both types contain two zero-amplitude points while as the increase of $\kappa$, the two maximum points move toward each other and eventually merge into a single point, generating a rogue wave resembling the Peregrine soliton (see figures 3(c) and (f)). In addition, figure 3 also indicates that the value of $\kappa$ influences the duration of rogue wave, which decreases as $\kappa$ ($> 0$) increases.

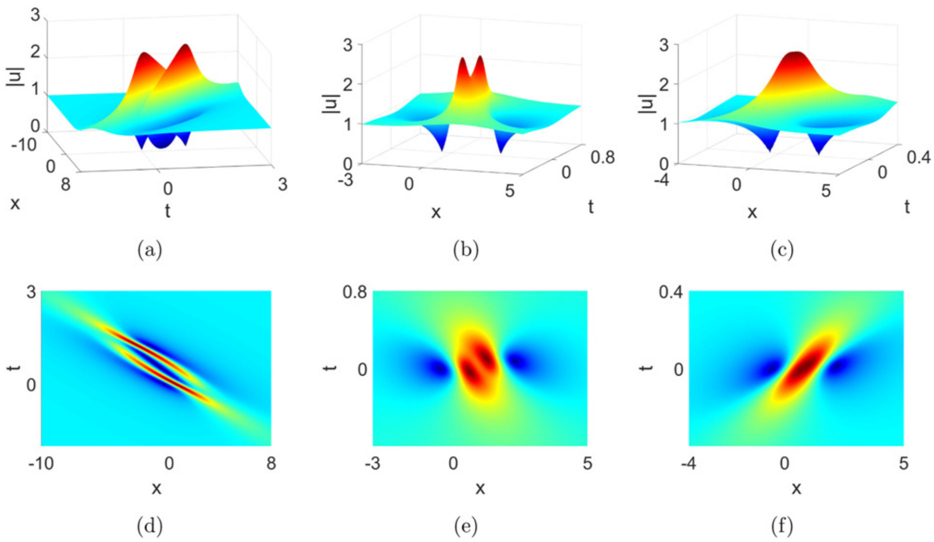


**Figure 3.** First-order rouge waves under parameter values $c = -0.5, a_0^{(0)} = 1, a_1^{(0)} = 0$ (a) $a = 0.5\mathrm{i}$, (c) $a = 1.04\mathrm{i}$ and (e) $a = 1.84\mathrm{i}$. (d), (e) and (f) are the corresponding density plots of (a), (b) and (c) respectively.

Finally, we discuss the reduction of first-order rogue wave solutions of the SS equation. Let $c = -1$ and apply the transformation

$$u(x,t) = q(\tau, z)\exp\left\{-\frac{\mathrm{i}}{6\varepsilon}\left(\tau - \frac{z}{18\varepsilon}\right)\right\}, \tag{50}$$

where $x = \tau - z/(12\epsilon)$, $t = -\epsilon z$, then the SS equation (equation (1) with $\beta_1 = 1$, $\beta_2 = 6$, $\beta_3 = 3$) reduces to the NLS equation

$$\mathrm{i}\frac{\partial q}{\partial z} + \frac{1}{2}\frac{\partial^2 q}{\partial \tau^2} + |q|^2 q = 0, \tag{51}$$

by taking the limit $\epsilon \to 0$. Furthermore, we take $\kappa = -1/(6\epsilon)$. As $\epsilon \to 0$, the solution (26) reduces to the following solution of the NLS equation

$$q(\tau, z) = \mathrm{e}^{\mathrm{i}z}\left(-1 + \frac{2 + 4\mathrm{i}z}{2\tau^2 + 2z^2 - 2\tau + 1}\right), \tag{52}$$

which is the so-called Peregrine soliton [19] with maximum amplitude 3 that is attained at $(\tau, z) = (1/2, 0)$ and two zero-amplitude points located at $(\tau, z) = ((1 \pm \sqrt{3})/2, 0)$. Clearly this indicates that the Peregrine soliton is the limiting case of rogue wave solutions of the SS equation.

## 4. Second-order rogue wave and its dynamics

The tau function for second-order rogue wave is a $4 \times 4$ determinant

$$\tau_{kl} = \begin{vmatrix} M_{11}^{kl} & M_{12}^{kl} \\ M_{21}^{kl} & M_{22}^{kl} \end{vmatrix}_{\substack{p_1 = q_1 = \xi \\ p_2 = q_2 = \xi^*}}, \tag{53}$$

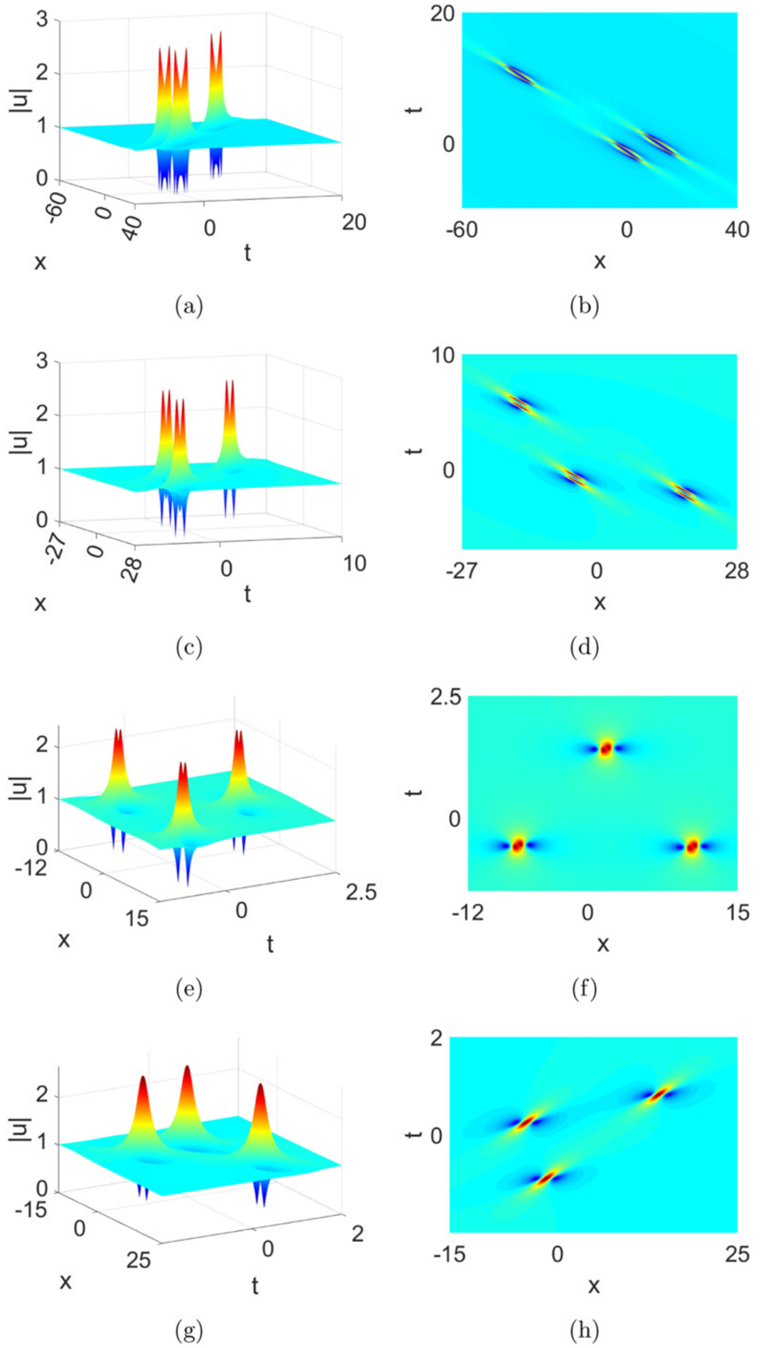


**Figure 4.** Second-order rouge waves under parameter values $a_0^{(0)} = 6, a_1^{(0)} = 0, a_2^{(0)} = 0$ and (a) $a = 0.45\mathrm{i},\ c = -0.5,\ a_3^{(0)} = 500$, (c) $a = 0.6\mathrm{i},\ c = -0.5,\ a_3^{(0)} = 1200$, (e) $a = 1.5\mathrm{i},\ c = -0.75,\ a_3^{(0)} = 10\,000\mathrm{i}$ and (g) $a = 2\mathrm{i},\ c = -0.5,\ a_3^{(0)} = 12\,000$. (b), (d), (f) and (h) are the corresponding density plots of (a), (c), (e) and (h) respectively.

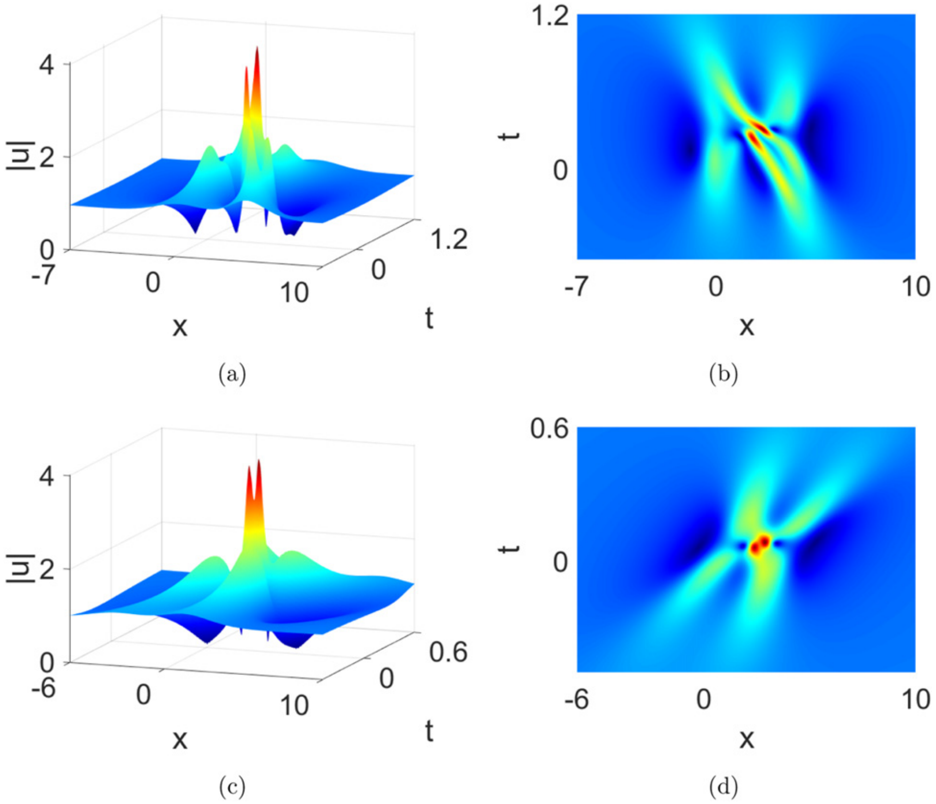


**Figure 5.** Second-order rouge waves under parameter values $a_0^{(0)} = 6, a_1^{(0)} = 0, a_2^{(0)} = 0$ and (a) $a = 1.04\mathrm{i}$, $c = -0.5$, $a_3^{(0)} = 31.569 + 10.197\mathrm{i}$ and (c) $a = 1.84\mathrm{i}$, $c = -0.5$, $a_3^{(0)} = 37.429 + 50.852\mathrm{i}$. (b) and (d) are the corresponding density plots of (a) and (c) respectively.

with

$$M_{ij}^{kl} = \begin{pmatrix} A_{2i-1}^{(N-i)}(p_1)B_{2j-1}^{(N-j)}(q_1)m_{11}^{kl} & A_{2i-1}^{(N-i)}(p_1)B_{2j-1}^{(N-j)}(q_2)m_{12}^{kl} \\ A_{2i-1}^{(N-i)}(p_2)B_{2j-1}^{(N-j)}(q_1)m_{21}^{kl} & A_{2i-1}^{(N-i)}(p_2)B_{2j-1}^{(N-j)}(q_2)m_{22}^{kl} \end{pmatrix}, \tag{54}$$

where

$$\begin{aligned}
&A_1^{(1)}(p) = a_0^{(1)} p\partial_p + a_1^{(1)}, \qquad B_1^{(1)}(q) = b_0^{(1)} q\partial_q + b_1^{(1)}, \\
&A_3^{(0)}(p) = \sum_{n=0}^{3} \frac{a_n^{(0)}}{(3-n)!}(p\partial_p)^{3-n}, \qquad B_3^{(0)}(q) = \sum_{n=0}^{3} \frac{b_n^{(0)}}{(3-n)!}(q\partial_q)^{3-n}, \\
&a_1^{(1)} = \sum_{n=0}^{2} \frac{F_{3-n}(p)}{(3-n)!} a_n^{(0)}, \qquad b_1^{(1)} = \sum_{n=0}^{2} \frac{F_{3-n}(q)}{(3-n)!} b_n^{(0)}, \\
&a_0^{(1)} = \sum_{n=0}^{1} \frac{F_{2-n}(p)}{(2-n)!} a_n^{(0)}, \qquad b_0^{(1)} = \sum_{n=0}^{1} \frac{F_{2-n}(q)}{(2-n)!} b_n^{(0)},
\end{aligned} \tag{55}$$

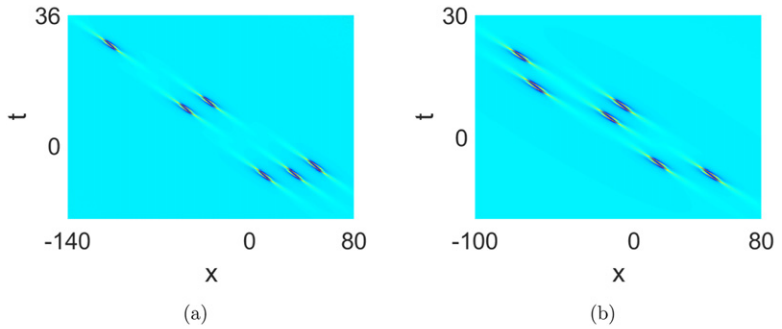


**Figure 6.** Third-order rouge waves with parameter values $a = 0.45\mathrm{i}$, $c = -0.5$, $a_0^{(0)} = 120$, $a_1^{(0)} = a_2^{(0)} = a_4^{(0)} = 0$ and (a) $a_3^{(0)} = 50\,000$, $a_5^{(0)} = 0$, (b) $a_3^{(0)} = 0$, $a_5^{(0)} = 1000\,000$.

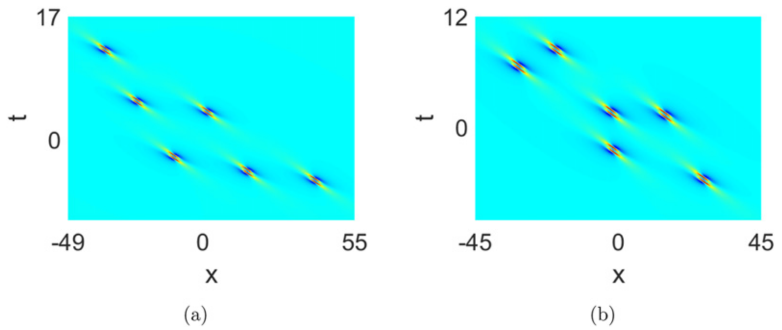


**Figure 7.** Third-order rouge waves with parameter values $a = 0.6\mathrm{i}$, $c = -0.5$, $a_0^{(0)} = 120$, $a_1^{(0)} = a_2^{(0)} = a_4^{(0)} = 0$ and (a) $a_3^{(0)} = 50\,000$, $a_5^{(0)} = 0$, (b) $a_3^{(0)} = 0$, $a_5^{(0)} = 1000\,000$.

and $p_i, q_j, \xi_{i0}, \eta_{j0}, a_n^{(0)}, b_n^{(0)}$ are constants that satisfy the same constraints as the first-order rogue waves. It is easily shown that the following relations hold

$$\widetilde{D}_{r,s,x} A_1^{(1)}(p_\alpha) B_1^{(1)}(q_\beta) m_{\alpha\beta}^{kl}\Big|_{\substack{p_1=q_1=\xi \\ p_2=q_2=\xi^*}} = [F(p_\alpha) + F(q_\beta)] A_1^{(1)}(p_\alpha) B_1^{(1)}(q_\beta) m_{\alpha\beta}^{kl}\Big|_{\substack{p_1=q_1=\xi \\ p_2=q_2=\xi^*}},$$

$$\widetilde{D}_{r,s,x} A_1^{(1)}(p_\alpha) B_3^{(0)}(q_\beta) m_{\alpha\beta}^{kl}\Big|_{\substack{p_1=q_1=\xi \\ p_2=q_2=\xi^*}} = [F(p_\alpha) + F(q_\beta)] A_1^{(1)}(p_\alpha) B_3^{(0)}(q_\beta) m_{\alpha\beta}^{kl} + A_1^{(1)}(p_\alpha) B_1^{(1)}(q_\beta) m_{\alpha\beta}^{kl}\Big|_{\substack{p_1=q_1=\xi \\ p_2=q_2=\xi^*}},$$

$$\widetilde{D}_{r,s,x} A_3^{(0)}(p_\alpha) B_1^{(1)}(q_\beta) m_{\alpha\beta}^{kl}\Big|_{\substack{p_1=q_1=\xi \\ p_2=q_2=\xi^*}} = [F(p_\alpha) + F(q_\beta)] A_3^{(0)}(p_\alpha) B_1^{(1)}(q_\beta) m_{\alpha\beta}^{kl} + A_1^{(1)}(p_\alpha) B_1^{(1)}(q_\beta) m_{\alpha\beta}^{kl}\Big|_{\substack{p_1=q_1=\xi \\ p_2=q_2=\xi^*}},$$

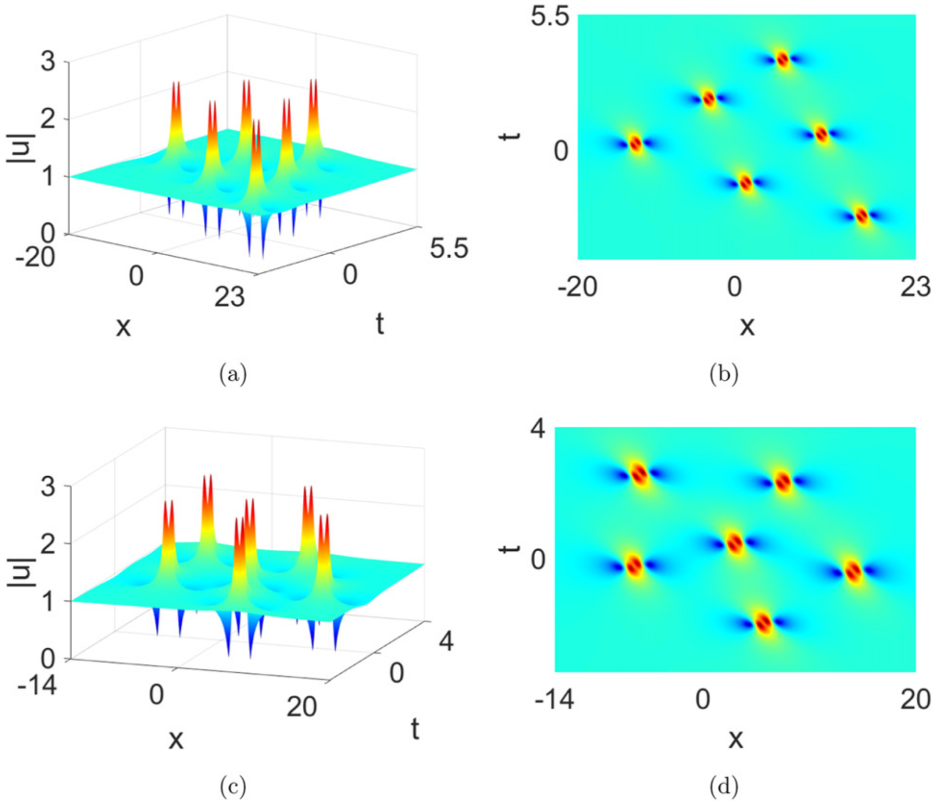


**Figure 8.** Third-order rouge waves with parameter values $a = 1.04\mathrm{i}, c = -0.5$, $a_0^{(0)} = 120$, $a_1^{(0)} = a_2^{(0)} = a_4^{(0)} = 0$ and (a) $a_3^{(0)} = 50\,000$, $a_5^{(0)} = 0$ and (c) $a_3^{(0)} = 0$, $a_5^{(0)} = 1000\,000$. (b) and (d) are the corresponding density plots of (a) and (c) respectively.

$$\widetilde{D}_{r,s,x} A_3^{(0)}(p_\alpha) B_3^{(0)}(q_\beta) m_{\alpha\beta}^{kl} \Big|_{\substack{p_1=q_1=\xi \\ p_2=q_2=\xi^*}} = [F(p_\alpha) + F(q_\beta)] A_3^{(0)}(p_\alpha) B_3^{(0)}(q_\beta) m_{\alpha\beta}^{kl} + A_1^{(1)}(p_\alpha) B_3^{(0)}(q_\beta) m_{\alpha\beta}^{kl} + A_3^{(0)}(p_\alpha) B_1^{(1)}(q_\beta) m_{\alpha\beta}^{kl} \Big|_{\substack{p_1=q_1=\xi \\ p_2=q_2=\xi^*}}, \tag{56}$$

which lead to

$$\widetilde{D}_{r,s,x}\, \tau_{kl} \Big|_{\substack{p_1=q_1=\xi \\ p_2=q_2=\xi^*}} = 4\left[F(\xi) + F(\xi^*)\right] \tau_{kl} \Big|_{\substack{p_1=q_1=\xi \\ p_2=q_2=\xi^*}}. \tag{57}$$

Thus, the second-order rogue waves are approved. Let us show their dynamics. For simplicity, we may set

$$a_1^{(0)} = b_1^{(0)} = a_2^{(0)} = b_2^{(0)} = 0. \tag{58}$$

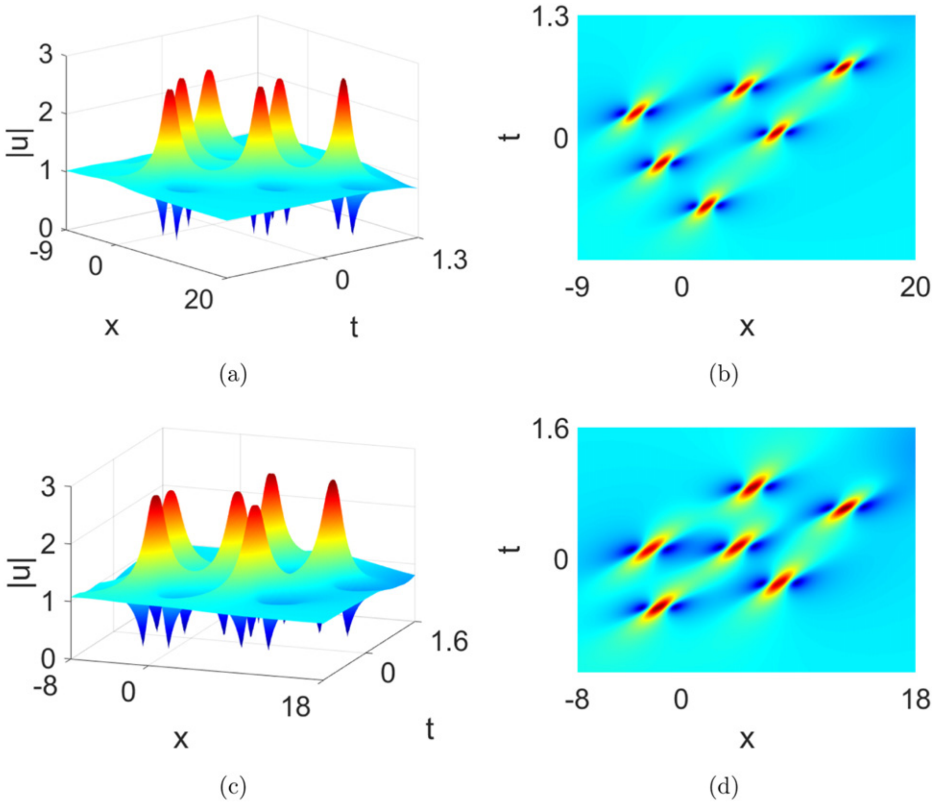


**Figure 9.** Third-order rouge waves with parameter values $a_0^{(0)} = 120$, $a_1^{(0)} = a_2^{(0)} = a_4^{(0)} = 0$ and (a) $a = 2.03\mathrm{i}$, $c = -0.65$, $a_3^{(0)} = 50\,000, a_5^{(0)} = 0$ and (c) $a = 1.84\mathrm{i}$, $c = -0.5$, $a_3^{(0)} = 0$, $a_5^{(0)} = 1000\,000$. (b) and (d) are the corresponding density plots of (a) and (c) respectively.

Recently Yang and Yang [32, 33] have systematically studied the rogue wave patterns of several integrable equations such as the NLS equation, the Bossinesq equation and the Manakov system. To be more precise, they have shown that when one of the internal parameters in the rogue wave solutions is large enough, by studying the asymptotic behaviors of solutions, the rogue wave patterns can be described by the root structure of the Yablonskii–Vorob'ev polynomial hierarchy via certain linear transformation. In particular, they have shown that the second-order rogue wave may consist of three separating fundamental rogue waves which are far away from the origin. It turns out that this also occurs in the second-order rogue wave solutions of the SS equation. As shown in figure 4, the second-order rogue waves contain three fundamental rogue waves which separate from each other when $a_3^{(0)}$ is large enough. As there are four types of fundamental rogue waves, we have totally four types of second-order rogue waves that contain three separating fundamental rogue waves. On the other hand, when $a_3^{(0)}$ is small, the three fundamental rogue waves may merge together (see figure 5). In addition, the argument of $a_3^{(0)}$ strongly affects the orientation of these rogue waves while the values of $a$ and $c$ determine the type and duration of rogue waves.

Similar to the first-order rogue wave solutions, with $\kappa = -1/(6\epsilon)$, the second-order rogue wave solutions of the SS equation degenerate to the second-order rogue wave solutions of the

NLS equation as $\epsilon \to 0$. It is also noted that the corresponding tau functions of these rogue wave solutions are polynomials of degree 12 in $x$ and $t$ whereas the second-order rogue wave solutions of the NLS equation have a much simpler structure as their $\tau$-functions are of degree 6 in $x$ and $t$ [37].

## 5. Third-order rogue wave and its dynamics

The tau function associated to the third-order rogue wave solution of the SS equation (4) is a $6 \times 6$ determinant

$$\tau_{kl} = \left. \begin{vmatrix} M_{11}^{kl} & M_{12}^{kl} & M_{13}^{kl} \\ M_{21}^{kl} & M_{22}^{kl} & M_{23}^{kl} \\ M_{31}^{kl} & M_{32}^{kl} & M_{33}^{kl} \end{vmatrix} \right|_{\substack{p_1=q_1=\xi \\ p_2=q_2=\xi^*}}, \tag{59}$$

with

$$M_{ij}^{kl} = \begin{pmatrix} A_{2i-1}^{(N-i)}(p_1)B_{2j-1}^{(N-j)}(q_1)m_{11}^{kl} & A_{2i-1}^{(N-i)}(p_1)B_{2j-1}^{(N-j)}(q_2)m_{12}^{kl} \\ A_{2i-1}^{(N-i)}(p_2)B_{2j-1}^{(N-j)}(q_1)m_{21}^{kl} & A_{2i-1}^{(N-i)}(p_2)B_{2j-1}^{(N-j)}(q_2)m_{22}^{kl} \end{pmatrix}. \tag{60}$$

The corresponding differential operators are defined as follows

$$\begin{aligned}
&A_1^{(2)} = a_0^{(2)} p\partial_p + a_1^{(2)}, && B_1^{(2)} = b_0^{(2)} q\partial_q + b_1^{(2)}, \\
&A_3^{(1)} = \sum_{n=0}^{3} \frac{a_n^{(1)}}{(3-n)!}(p\partial_p)^{3-n}, && B_3^{(1)} = \sum_{n=0}^{3} \frac{b_n^{(1)}}{(3-n)!}(q\partial_q)^{3-n}, \\
&A_5^{(0)} = \sum_{n=0}^{5} \frac{a_n^{(0)}}{(5-n)!}(p\partial_p)^{5-n}, && B_5^{(0)} = \sum_{n=0}^{5} \frac{b_n^{(0)}}{(5-n)!}(q\partial_q)^{5-n}, \\
&a_1^{(2)} = \sum_{n=0}^{1} \frac{F_{3-n}(p)}{(3-n)!} a_n^{(1)}, && b_1^{(2)} = \sum_{n=0}^{1} \frac{F_{3-n}(q)}{(3-n)!} b_n^{(1)}, \\
&a_0^{(2)} = \frac{a_n^{(1)}}{(2-n)!} F_{2-n}(p), && b_0^{(2)} = \sum_{n=0}^{0} \frac{b_n^{(1)}}{(2-n)!} F_{2-n}(q), \\
&a_0^{(1)} = \sum_{n=2}^{2} \frac{1}{n!} a_{2-n}^{(0)} F_n(p), && b_0^{(1)} = \sum_{n=2}^{2} \frac{1}{n!} b_{2-n}^{(0)} F_n(q), \\
&a_1^{(1)} = \sum_{n=2}^{3} \frac{1}{n!} a_{3-n}^{(0)} F_n(p), && b_1^{(1)} = \sum_{n=2}^{3} \frac{1}{n!} b_{3-n}^{(0)} F_n(q), \\
&a_2^{(1)} = \sum_{n=2}^{4} \frac{1}{n!} a_{4-n}^{(0)} F_n(p), && b_2^{(1)} = \sum_{n=2}^{4} \frac{1}{n!} b_{4-n}^{(0)} F_n(q), \\
&a_3^{(1)} = \sum_{n=2}^{5} \frac{1}{n!} a_{5-n}^{(0)} F_n(p), && b_3^{(1)} = \sum_{n=2}^{5} \frac{1}{n!} b_{5-n}^{(0)} F_n(q).
\end{aligned} \tag{61}$$

It can be shown that ($i, j = 2, 3,\ \mu, \nu = 0, 1$)

$$\widetilde{D}_{r,s,x} A_1^{(2)}(p_\alpha) B_1^{(2)}(q_\beta) m_{\alpha\beta}^{kl}\Big|_{\substack{p_1=q_1=\xi\\ p_2=q_2=\xi^*}} = [F(p_\alpha)+F(q_\beta)] A_1^{(2)}(p_\alpha) B_1^{(2)}(q_\beta) m_{\alpha\beta}^{kl}\Big|_{\substack{p_1=q_1=\xi\\ p_2=q_2=\xi^*}},$$

$$\widetilde{D}_{r,s,x} A_1^{(2)}(p_\alpha) B_{2j-1}^{(\nu)}(q_\beta) m_{\alpha\beta}^{kl}\Big|_{\substack{p_1=q_1=\xi\\ p_2=q_2=\xi^*}} = [F(p_\alpha)+F(q_\beta)] A_1^{(2)}(p_\alpha) B_{2j-1}^{(\nu)}(q_\beta) m_{\alpha\beta}^{kl} + A_1^{(2)}(p_\alpha) B_{2j-3}^{(\nu+1)}(q_\beta) m_{\alpha\beta}^{kl}\Big|_{\substack{p_1=q_1=\xi\\ p_2=q_2=\xi^*}},$$

$$\widetilde{D}_{r,s,x} A_{2i-1}^{(\mu)}(p_\alpha) B_1^{(2)}(q_\beta) m_{\alpha\beta}^{kl}\Big|_{\substack{p_1=q_1=\xi\\ p_2=q_2=\xi^*}} = [F(p_\alpha)+F(q_\beta)] A_{2i-1}^{(\mu)}(p_\alpha) B_1^{(2)}(q_\beta) m_{\alpha\beta}^{kl} + A_{2i-3}^{(\mu+1)}(p_\alpha) B_1^{(2)}(q_\beta) m_{\alpha\beta}^{kl}\Big|_{\substack{p_1=q_1=\xi\\ p_2=q_2=\xi^*}},$$

$$\widetilde{D}_{r,s,x} A_{2i-1}^{(\mu)}(p_\alpha) B_{2j-1}^{(\nu)}(q_\beta) m_{\alpha\beta}^{kl}\Big|_{\substack{p_1=q_1=\xi\\ p_2=q_2=\xi^*}} = [F(p_\alpha)+F(q_\beta)] A_{2i-1}^{(\mu)}(p_\alpha) B_{2j-1}^{(\nu)}(q_\beta) m_{\alpha\beta}^{kl} + A_{2i-3}^{(\mu+1)}(p_\alpha) B_{2j-1}^{(\nu)}(q_\beta) m_{\alpha\beta}^{kl} + A_{2i-1}^{(\mu)}(p_\alpha) B_{2j-3}^{(\nu+1)}(q_\beta) m_{\alpha\beta}^{kl}\Big|_{\substack{p_1=q_1=\xi\\ p_2=q_2=\xi^*}}. \tag{62}$$

Based on above relations, we can verify

$$\widetilde{D}_{r,s,x}\, \tau_{kl}\Big|_{\substack{p_1=q_1=\xi\\ p_2=q_2=\xi^*}} = 6\left[F(\xi)+F(\xi^*)\right] \tau_{kl}\Big|_{\substack{p_1=q_1=\xi\\ p_2=q_2=\xi^*}}, \tag{63}$$

which completes the proof. With the explicit third-order rogue wave solutions, we can explore their dynamics in detail. For the NLS equation, it has been shown graphically by Ohta and Yang [37] that its third-order rogue waves may be comprised of six individual first-order rogue waves. In this case, there are two possible configurations: one is a symmetric triangle while the other is like a pentagon. The analytic proof of these patterns is given by Yang and Yang [32] by connecting rogue wave solutions of the NLS equation with the root structure of the Yablonskii–Vorob'ev polynomial hierarchy and assuming certain parameter is large enough. Surprisingly, these patterns also appear in the third-order rogue wave solutions of many other integrable systems [33]. Since the NLS equation is a limiting case of the SS equation, we may expect that the SS equation shares analogous features. As depicted in figures 6–9, this is indeed the case.

Our computation indicates that the corresponding tau functions of third-order rogue wave solutions are polynomials of degree 24 in $x$ and $t$, which are much more complicated than the tau functions (degree 12 in $x$ and $t$) of third-order rogue waves of the NLS equation. Therefore, in addition to the two configurations, four types of intrinsic structures occur in the third-order rogue waves of the SS equation as shown in figures 6–9. When $a_0^{(0)} = 120$, $a_3^{(0)}$ is large enough and other parameters are zero, the third-order rogue wave consists of six first-order rogue waves that feature a triangle. In contrast, when $a_0^{(0)} = 120$, $a_5^{(0)}$ is large enough and other parameters are zero, the third-order rogue waves are comprised of six first-order rogue waves which constitute a distorted pentagon. It can also be seen from figures 6–9 that the degree of distortion depends on the values of the parameter $a$ which also affects the type and duration of rogue waves.

## 6. Conclusions

In the present paper, the rogue wave solutions are shown to exist for the SS equation (4) when $c < 0$ and are constructed by means of Hirota's bilinear method. We have presented the first-, second- and third-order rogue wave solutions of the SS equation in explicit forms. In particular, we have confirmed that the TRW and four types of intrinsic structures exist in all orders of rogue wave solutions of the SS equation. While the explicit first- and second-order rogue wave solutions have been reported previously, to the best of our knowledge, the explicit expressions of the third-order rogue wave solutions are relatively new. We have shown that the degree of the tau functions corresponding to the third-order rogue wave solutions is 24, which is much higher than that of the NLS equation (degree 12). We have also shown that there are totally four types of third-order rogue waves consisting of six individual first-order rogue waves, and each type can be classified into two patterns. One pattern is a triangle whereas the other is a distorted pentagon. The types of rogue waves and the degree of distortion of the pentagons are determined by the choices of free parameters in the solutions. In addition, the degeneration of first-order rogue wave solutions of the SS equation to its limiting case, the NLS equation, was discussed in detail. This indicates that the rogue wave solutions of the SS equation are generalizations of rogue wave solutions of the NLS equation. We expect that the results obtained in this work could deepen our understanding on rogue waves in the deep ocean or optical fibers. As a further topic, we will explore the $N$th-order rogue wave solutions of the SS equation and their universal patterns.

## Acknowledgments

The authors would like to thank the anonymous reviewers for their valuable comments and suggestions to improve the quality of the paper. We would also like to thank Mr Peng Huang for the helpful discussions. B F Feng was partially supported by National Science Foundation (NSF) under Grant No. DMS-1715991 and US Department of Defense (DoD), Air Force for Scientific Research (AFOSR) under Grant No. W911NF2010276. C F Wu was supported by the National Natural Science Foundation of China (Grant Nos. 11701382 and 11971288) and Guangdong Basic and Applied Basic Research Foundation, China (Grant No. 2021A1515010054).

## Data availability statement

The data that support the findings of this study are available upon reasonable request from the authors.

## Appendix A

In this appendix, we show that the function $\tau_{kl}$ defined in (13) satisfies eleven bilinear equations. To this end, we first introduce a crucial lemma.

**Lemma 1.** *Suppose $m_{ij}^{kl}, \varphi_i^{kl}, \psi_j^{kl}$, which are functions of $x, y, t, r, s$, satisfy the differential and difference relations*

$$\partial_x m_{ij}^{kl} = \varphi_i^{kl}\psi_j^{k,l}, \tag{64}$$

$$\partial_x \varphi_i^{k,l} = \varphi_i^{k+1,l} + a\varphi_i^{k,l} = \varphi_i^{k,l+1} + b\varphi_i^{k,l}, \tag{65}$$

$$\partial_x \psi_j^{k,l} = -\psi_j^{k-1,l} - a\psi_j^{k,l} = -\psi_j^{k,l-1} - b\psi_j^{k,l}, \tag{66}$$

$$\partial_y \varphi_i^{k,l} = \partial_x^2 \varphi_i^{k,l}, \qquad \partial_y \psi_j^{k,l} = -\partial_x^2 \psi_j^{k,l}, \tag{67}$$

$$\partial_t \varphi_i^{k,l} = \partial_x^3 \varphi_i^{k,l}, \qquad \partial_t \psi_j^{k,l} = \partial_x^3 \psi_j^{k,l}, \tag{68}$$

$$\partial_r \varphi_i^{k,l} = \varphi_i^{k-1,l}, \qquad \partial_r \psi_j^{k,l} = -\psi_j^{k+1,l}, \tag{69}$$

$$\partial_s \varphi_i^{k,l} = \varphi_i^{k,l-1}, \qquad \partial_s \psi_j^{k,l} = -\psi_j^{k,l+1}, \tag{70}$$

*which imply the relations*

$$\begin{aligned}\partial_y m_{ij}^{kl} &= \varphi_i^{k+1,l}\psi_j^{kl} + \varphi_i^{kl}\psi_j^{k-1,l} + 2a\varphi_i^{kl}\psi_j^{kl} \\ &= \varphi_i^{k,l+1}\psi_j^{kl} + \varphi_i^{kl}\psi_j^{k,l-1} + 2b\varphi_i^{kl}\psi_j^{kl},\end{aligned} \tag{71}$$

$$\begin{aligned}\partial_t m_{ij}^{kl} &= \varphi_i^{k+2,l}\psi_j^{kl} + 3a\varphi_i^{k+1,l}\psi_j^{k,l} + \varphi_i^{k+1,l}\psi_j^{k-1,l} \\ &\quad + 3a^2\varphi_i^{kl}\psi_j^{kl} + 3a\varphi_i^{kl}\psi_j^{k-1,l} + \varphi_i^{kl}\psi_j^{k-2,l},\end{aligned} \tag{72}$$

$$\begin{aligned}&= \varphi_i^{k,l+2}\psi_j^{kl} + 3b\varphi_i^{k,l+1}\psi_j^{kl} + \varphi_i^{k,l+1}\psi_j^{k,l-1} \\ &\quad + 3b^2\varphi_i^{kl}\psi_j^{kl} + 3b\varphi_i^{kl}\psi_j^{k,l-1} + \varphi_i^{kl}\psi_j^{k,l-2},\end{aligned} \tag{73}$$

$$\partial_r m_{ij}^{kl} = -\varphi_i^{k-1,l}\psi_j^{k+1,l}, \partial_s m_{ij}^{kl} = -\varphi_i^{k,l-1}\psi_j^{k,l+1}, \tag{74}$$

$$m_{ij}^{k+1,l} = m_{ij}^{kl} + \varphi_i^{kl}\psi_j^{k+1,l}, \qquad m_{ij}^{k,l+1} = m_{ij}^{kl} + \varphi_i^{kl}\psi_j^{k,l+1}, \tag{75}$$

*then the determinant*

$$\tau_{kl} = \det_{1\leqslant i,j\leqslant N}\left(m_{ij}^{kl}\right), \tag{76}$$

*satisfies the following bilinear equations in the KP hierarchy*

$$(D_r D_x - 2)\,\tau_{kl}\cdot\tau_{kl} = -2\tau_{k+1,l}\tau_{k-1,l}, \tag{77}$$

$$(D_s D_x - 2)\,\tau_{kl}\cdot\tau_{kl} = -2\tau_{k,l+1}\tau_{k,l-1}, \tag{78}$$

$$\left(D_x^2 - D_y + 2aD_x\right)\tau_{k+1,l}\cdot\tau_{kl} = 0, \tag{79}$$

$$\left(D_x^2 - D_y + 2bD_x\right)\tau_{k,l+1}\cdot\tau_{kl} = 0, \tag{80}$$

$$\left(D_x^3 + 3D_xD_y - 4D_t + 3a\left(D_x^2 + D_y\right) + 6a^2D_x\right)\tau_{k+1,l}\cdot\tau_{kl} = 0, \tag{81}$$

$$\left(D_x^3 + 3D_xD_y - 4D_t + 3b\left(D_x^2 + D_y\right) + 6b^2D_x\right)\tau_{k,l+1}\cdot\tau_{kl} = 0, \tag{82}$$

$$\left(D_r\left(D_x^2 - D_y + 2aD_x\right) - 4D_x\right)\tau_{k+1,l}\cdot\tau_{kl} = 0, \tag{83}$$

$$\left(D_s\left(D_x^2 - D_y + 2bD_x\right) - 4D_x\right)\tau_{k,l+1}\cdot\tau_{kl} = 0, \tag{84}$$

$$\left(D_s\left(D_x^2 - D_y + 2aD_x\right) - 4\left(D_x + a - b\right)\right)\tau_{k+1,l}\cdot\tau_{kl} + 4(a-b)\tau_{k+1,l+1}\tau_{k,l-1} = 0, \tag{85}$$

$$\left(D_r\left(D_x^2 - D_y + 2bD_x\right) - 4\left(D_x + b - a\right)\right)\tau_{k,l+1}\cdot\tau_{kl} + 4(b-a)\tau_{k+1,l+1}\tau_{k-1,l} = 0, \tag{86}$$

$$\left(D_x + a - b\right)\tau_{k+1,l}\cdot\tau_{k,l+1} = (a-b)\tau_{k+1,l+1}\tau_{kl}. \tag{87}$$

**Proof.** The proof of this lemma is based on properties of the Gram-type determinant [56]. For convenience, we only prove the $\tau_{kl}$ defined in (13) satisfies the bilinear equation (87) as other cases can be treated by using similar techniques.

We first recall two properties of determinants, i.e.,

$$\partial_x \det_{1\leqslant i,j\leqslant N}\left(a_{ij}\right) = \sum_{i,j=1}^{N}\Delta_{ij}\partial_x a_{ij}, \tag{88}$$

and

$$\det\begin{pmatrix} a_{ij} & b_i \\ c_j & d\end{pmatrix} = -\sum_{i,j}\Delta_{ij}b_ic_j + d\,\det\left(a_{ij}\right), \tag{89}$$

where $\Delta_{ij}$ is the $(i, j)$-cofactor of the matrix $(a_{ij})$. By using these properties, we may rewrite the derivatives and shifts of the $\tau$ function as below

$$\tau_{k+1,l} = \begin{vmatrix} m_{ij}^{kl} & \varphi_i^{kl} \\ -\psi_j^{k+1,l} & 1\end{vmatrix}, \tag{90}$$

$$\tau_{k,l+1} = \begin{vmatrix} m_{ij}^{kl} & \varphi_i^{kl} \\ -\psi_j^{k,l+1} & 1\end{vmatrix} = \begin{vmatrix} m_{ij}^{kl} & \varphi_i^{kl} \\ -\psi_j^{k,l+1} & 0\end{vmatrix} + \tau_{kl}, \tag{91}$$

$$\partial_x\tau_{k+1,l} = \begin{vmatrix} m_{ij}^{kl} & \varphi_i^{k+1,l} \\ -\psi_j^{k+1,l} & 0\end{vmatrix} = \begin{vmatrix} m_{ij}^{k+1,l} & \varphi_i^{k+1,l} \\ -\psi_j^{k+1,l} & 0\end{vmatrix}, \tag{92}$$

$$\partial_x\tau_{k,l+1} = \begin{vmatrix} m_{ij}^{kl} & \varphi_i^{k+1,l} \\ -\psi_j^{k,l+1} & 0\end{vmatrix} + \begin{vmatrix} m_{ij}^{kl} & \varphi_i^{kl} \\ -\psi_j^{kl} & 0\end{vmatrix} + \begin{vmatrix} m_{ij}^{kl} & \varphi_i^{kl} \\ -\psi_j^{k-1,l+1} & 0\end{vmatrix}, \tag{93}$$

$$\tau_{k+1,l+1} = \begin{vmatrix} m_{ij}^{k+1,l} & \varphi_i^{k+1,l} \\ -\psi_j^{k+1,l+1} & 0 \end{vmatrix} + \tau_{k+1,l}. \tag{94}$$

Then it follows from the identities above and equation (66) that

$$\begin{aligned}
&(a-b)(\tau_{k+1,l+1}\cdot\tau_{kl} - \tau_{k+1,l}\cdot\tau_{k,l+1}) \\
&= \begin{vmatrix} m_{ij}^{k+1,l} & \varphi_i^{k+1,l} \\ \psi_j^{k,l+1} & 0 \end{vmatrix}\cdot\tau_{kl} + \begin{vmatrix} m_{ij}^{k+1,l} & \varphi_i^{k+1,l} \\ -\psi_j^{k+1,l} & 0 \end{vmatrix}\cdot\tau_{kl} \\
&\quad - \begin{vmatrix} m_{ij}^{kl} & \varphi_i^{kl} \\ -\psi_j^{kl} & 0 \end{vmatrix}\cdot\tau_{k+1,l} - \begin{vmatrix} m_{ij}^{kl} & \varphi_i^{kl} \\ \psi_j^{k-1,l+1} & 0 \end{vmatrix}\cdot\tau_{k+1,l} \\
&= \begin{vmatrix} m_{ij}^{kl} & \varphi_i^{kl} & \varphi_i^{k+1,l} \\ -\psi_j^{k,l+1} & 0 & 0 \\ -\psi_j^{k+1,l} & 1 & 0 \end{vmatrix}\cdot\tau_{kl} + \begin{vmatrix} m_{ij}^{k+1,l} & \varphi_i^{k+1,l} \\ -\psi_j^{k+1,l} & 0 \end{vmatrix}\cdot\tau_{kl} \\
&\quad - \begin{vmatrix} m_{ij}^{kl} & \varphi_i^{kl} \\ -\psi_j^{kl} & 0 \end{vmatrix}\cdot\tau_{k+1,l} - \begin{vmatrix} m_{ij}^{kl} & \varphi_i^{kl} \\ \psi_j^{k-1,l+1} & 0 \end{vmatrix}\cdot\tau_{k+1,l},
\end{aligned} \tag{95}$$

and

$$\begin{aligned}
&\partial_x\tau_{k+1,l}\cdot\tau_{k,l+1} - \tau_{k+1,l}\cdot\partial_x\tau_{k,l+1} \\
&= \begin{vmatrix} m_{ij}^{kl} & \varphi_i^{k+1,l} \\ -\psi_j^{k+1,l} & 0 \end{vmatrix}\cdot\begin{vmatrix} m_{ij}^{kl} & \varphi_i^{kl} \\ \psi_j^{k,l+1} & 0 \end{vmatrix} + \begin{vmatrix} m_{ij}^{k+1,l} & \varphi_i^{k+1,l} \\ -\psi_j^{k+1,l} & 0 \end{vmatrix}\cdot\tau_{kl} \\
&\quad - \begin{vmatrix} m_{ij}^{kl} & \varphi_i^{k+1,l} \\ -\psi_j^{k,l+1} & 0 \end{vmatrix}\cdot\tau_{k+1,l} - \begin{vmatrix} m_{ij}^{kl} & \varphi_i^{kl} \\ -\psi_j^{kl} & 0 \end{vmatrix}\cdot\tau_{k+1,l} \\
&\quad - \begin{vmatrix} m_{ij}^{kl} & \varphi_i^{kl} \\ \psi_j^{k-1,l+1} & 0 \end{vmatrix}\cdot\tau_{k+1,l}.
\end{aligned} \tag{96}$$

Thus, by applying the Jacobi formula of determinants

$$\begin{vmatrix} a_{ij} & b_i & c_i \\ d_j & e & f \\ g_j & h & k \end{vmatrix}\times|a_{ij}| = \begin{vmatrix} a_{ij} & c_i \\ g_j & k \end{vmatrix}\times\begin{vmatrix} a_{ij} & b_i \\ d_j & e \end{vmatrix} - \begin{vmatrix} a_{ij} & b_i \\ g_j & h \end{vmatrix}\times\begin{vmatrix} a_{ij} & c_i \\ d_j & f \end{vmatrix}, \tag{97}$$

we may deduce that

$$\begin{aligned}
&(a-b)(\tau_{k+1,l+1}\cdot\tau_{kl} - \tau_{k+1,l}\cdot\tau_{k,l+1}) - (\partial_x\tau_{k+1,l}\cdot\tau_{k,l+1} - \tau_{k+1,l}\cdot\partial_x\tau_{k,l+1}) \\
&= \begin{vmatrix} m_{ij}^{kl} & \varphi_i^{kl} & \varphi_i^{k+1,l} \\ -\psi_j^{k,l+1} & 0 & 0 \\ -\psi_j^{k+1,l} & 1 & 0 \end{vmatrix}\left|m_{ij}^{kl}\right| \\
&\quad - \begin{vmatrix} m_{ij}^{kl} & \varphi_i^{k+1,l} \\ -\psi_j^{k+1,l} & 0 \end{vmatrix}\begin{vmatrix} m_{ij}^{kl} & \varphi_i^{kl} \\ \psi_j^{k,l+1} & 0 \end{vmatrix} \\
&\quad + \begin{vmatrix} m_{ij}^{kl} & \varphi_i^{kl} \\ -\psi_j^{k+1,l} & 1 \end{vmatrix}\begin{vmatrix} m_{ij}^{kl} & \varphi_i^{k+1,l} \\ -\psi_j^{k,l+1} & 0 \end{vmatrix} \\
&= 0.
\end{aligned} \tag{98}$$

This completes the proof. □

Denote by

$$m^{kl}_{\alpha\beta} = \frac{1}{p_\alpha + q_\beta}\left(-\frac{p_\alpha - a}{q_\beta + a}\right)^k \left(-\frac{p_\alpha - b}{q_\beta + b}\right)^l e^{\xi_\alpha + \eta_\beta}, \tag{99}$$

$$\varphi^{kl}_\alpha = (p_\alpha - a)^k (p_\alpha - b)^l e^{\xi_\alpha}, \tag{100}$$

$$\psi^{kl}_\beta = [-(q_\beta + a)]^{-k}[-(q_\beta + b)]^{-l} e^{\eta_\beta}, \tag{101}$$

$$\xi_\alpha = p_\alpha x + p_\alpha^2 y + p_\alpha^3 t + \frac{1}{p_\alpha - a} r + \frac{1}{p_\alpha - b} s + \xi_{\alpha 0}, \tag{102}$$

$$\eta_\beta = q_\beta x - q_\beta^2 y + q_\beta^3 t + \frac{1}{q_\beta + a} r + \frac{1}{q_\beta + b} s + \eta_{\beta 0}, \tag{103}$$

where $\alpha, \beta = 1, 2$, and $p_\alpha, q_\beta, \xi_{\alpha 0}, \eta_{\beta 0}$ are constants, then direct computations indicate that $m^{kl}_{\alpha\beta}, \varphi^{kl}_\alpha, \psi^{kl}_\beta$ satisfy the differential and difference relations (64)–(70).

Next, we define

$$M^{kl}_{ij} = \begin{pmatrix} \widetilde{m}^{kl}_{2i-1,2j-1} & \widetilde{m}^{kl}_{2i-1,2j} \\ \widetilde{m}^{kl}_{2i,2j-1} & \widetilde{m}^{kl}_{2i,2j} \end{pmatrix} = \begin{pmatrix} A_i(p_1)B_j(q_1)m^{kl}_{11} & A_i(p_1)B_j(q_2)m^{kl}_{12} \\ A_i(p_2)B_j(q_1)m^{kl}_{21} & A_j(p_2)B_j(q_2)m^{kl}_{22} \end{pmatrix},$$

and

$$\begin{pmatrix} \widetilde{\varphi}^{kl}_{2i-1} \\ \widetilde{\varphi}^{kl}_{2i} \end{pmatrix} = \begin{pmatrix} A_i(p_1)\varphi^{kl}_1 \\ A_i(p_2)\varphi^{kl}_2 \end{pmatrix},$$

$$\left(\widetilde{\psi}^{kl}_{2j-1}, \widetilde{\psi}^{kl}_{2j}\right) = \left(B_j(q_1)\psi^{kl}_1, B_j(q_2)\psi^{kl}_2\right),$$

where $i, j = 1, 2, \ldots, N$ and

$$A_i(p) = \sum_{n=0}^{i} \frac{a_{i-n}(p)}{n!}(p\partial_p)^n, \qquad B_j(q) = \sum_{n=0}^{j} \frac{b_{j-n}(q)}{n!}(q\partial_q)^n,$$

then the functions $\widetilde{m}^{kl}_{ij}, \widetilde{\varphi}^{kl}_i, \widetilde{\psi}^{kl}_j$ would satisfy the differential and difference relations (64)–(70) as the operators $A_i$ and $B_j$ commute with the partial differentials with respect to $x, y, t, r, s$. Hence, using lemma 1, we conclude that the determinant

$$\tau_{kl} = \det_{1 \leqslant \mu,\nu \leqslant N}\left(M^{kl}_{i_\mu j_\nu}\right), \tag{104}$$

satisfies the bilinear equations (77)–(87) for any sequence of indices $(i_1, i_2, \ldots, i_N; j_1, j_2, \ldots, j_N)$.

## ORCID iDs

Bao-Feng Feng https://orcid.org/0000-0002-2529-897X
Chengfa Wu https://orcid.org/0000-0003-1697-4654

## References

[1] Ablowitz M J and Clarkson P A 1991 *Solitons, Nonlinear Evolution Equations and Inverse Scattering* (Cambridge: Cambridge University Press)
[2] Ablowitz M J, Prinari B and Trubatch A D 2004 *Discrete and Continuous Nonlinear Schrödinger Systems* (Cambridge: Cambridge University Press)
[3] Agrawal G P 1995 *Nonlinear Fiber Optics* (New York: Academic)
[4] Hasegawa A and Kodama Y 1995 *Solitons in Optical Communications* (Oxford: Clarendon)
[5] Kivshar Y S and Agrawal G P 2003 *Optical Solitons: From Fibers to Photonic Crystals* (New York: Academic)
[6] Dalfovo F, Giorgini S, Pitaevskii L P and Stringari S 1999 Theory of Bose–Einstein condensation in trapped gases *Rev. Mod. Phys.* **71** 463
[7] Benney D J and Newell A C 1967 The propagation of nonlinear wave envelopes *J. Math. Phys.* **46** 133–9
[8] Zakharov V E 1972 Collapse of Langmuir waves *Sov. Phys. JETP* **35** 908–14
[9] Sasa N and Satsuma J 1991 New-type of soliton solutions for a higher-order nonlinear Schrödinger equation *J. Phys. Soc. Japan* **60** 409–17
[10] Gilson C, Hietarinta J, Nimmo J and Ohta Y 2003 Sasa–Satsuma higher-order nonlinear Schrödinger equation and its bilinearization and multisoliton solutions *Phys. Rev.* E **68** 016614
[11] Hirota R 1973 Exact envelope-soliton solutions of a nonlinear wave equation *J. Math. Phys.* **14** 805–9
[12] Solli D R, Ropers C, Koonath P and Jalali B 2007 Optical rogue waves *Nature* **450** 1054–7
[13] Dysthe K, Krogstad H E and Müller P 2008 Oceanic rogue waves *Annu. Rev. Fluid Mech.* **40** 287–310
[14] Chabchoub A, Hoffmann N P and Akhmediev N 2011 Rogue wave observation in a water wave tank *Phys. Rev. Lett.* **106** 204502
[15] Calini A and Schober C M 2012 Dynamical criteria for rogue waves in nonlinear Schrödinger models *Nonlinearity* **25** R99–116
[16] Calini A and Schober C M 2013 Observable and reproducible rogue waves *J. Opt.* **15** 105201
[17] Ablowitz M J and Horikis T P 2017 Rogue waves in birefringent optical fibers: elliptical and isotropic fibers *J. Opt.* **19** 065501
[18] Ablowitz M J and Cole J T 2021 Transverse instability of rogue waves *Phys. Rev. Lett.* **127** 104101
[19] Peregrine D H 1983 Water waves, nonlinear Schrödinger equations and their solutions *J. Aust. Math. Soc.* B **25** 16–43
[20] Akhmediev N, Ankiewicz A and Soto-Crespo J M 2009 Rogue waves and rational solutions of the nonlinear Schrödinger equation *Phys. Rev.* E **80** 026601
[21] He J S, Xu S and Porsezian K 2012 *N*-order bright and dark rogue waves in a resonant erbium-doped fiber system *Phys. Rev.* E **86** 066603
[22] Wu C F, Grimshaw R H J, Chow K W and Chan H N 2015 A coupled 'AB' system: rogue waves and modulation instabilities *Chaos* **25** 103113
[23] Ankiewicz A, Akhmediev N and Soto-Crespo J 2010 Discrete rogue waves of the Ablowitz–Ladik and Hirota equations *Phys. Rev.* E **82** 026602
[24] Baronio F, Conforti M, Degasperis A, Lombardo S, Onorato M and Wabnitz S 2014 Vector rogue waves and baseband modulation instability in the defocusing regime *Phys. Rev. Lett.* **113** 034101
[25] Chen S and Mihalache D 2015 Vector rogue waves in the Manakov system: diversity and compossibility *J. Phys. A: Math. Theor.* **48** 215202
[26] Yang J 2010 *Nonlinear Waves in Integrable and Nonintegrable Systems* (Philadelphia, PA: SIAM)
[27] Bilman D, Ling L and Miller P D 2020 Extreme superposition: rogue waves of infinite order and the Painlev-III hierarchy *Duke Math. J.* **169** 671–760
[28] Chen J and Pelinovsky D E 2018 Rogue periodic waves of the focusing nonlinear Schrödinger equation *Proc. R. Soc.* A **474** 20170814

[29] Chen J, Pelinovsky D E and White R E 2019 Rogue waves on the double-periodic background in the focusing nonlinear Schrödinger equation *Phys. Rev.* E **100** 052219
[30] Feng B F, Ling L and Takahashi D A 2020 Multi-breather and high-order rogue waves for the nonlinear Schrödinger equation on the elliptic function background *Stud. Appl. Math.* **144** 46–101
[31] Zhang H-Q and Chen F 2021 Rogue waves for the fourth-order nonlinear Schrödinger equation on the periodic background *Chaos* **31** 023129
[32] Yang B and Yang J 2021 Rogue wave patterns in the nonlinear Schrödinger equation *Physica* D **419** 132850
[33] Yang B and Yang J 2021 Universal rogue wave patterns associated with the Yablonskii–Vorob'ev polynomial hierarchy *Physica* D **425** 132958
[34] Degasperis A and Lombardo S 2013 Rational solitons of wave resonant-interaction models *Phys. Rev.* E **88** 052914
[35] Bandelow U and Akhmediev N 2012 Sasa–Satsuma equation: soliton on a background and its limiting cases *Phys. Rev.* E **86** 026606
[36] Hirota R 2004 *The Direct Method in Soliton Theory* (Cambridge: Cambridge University Press)
[37] Ohta Y and Yang J 2012 General high-order rogue waves and their dynamics in the nonlinear Schrödinger equation *Proc. R. Soc.* A **468** 1716–40
[38] Degasperis A, Lombardo S and Sommacal M 2018 Rogue wave type solutions and spectra of coupled nonlinear Schrödinger equations *Fluids* **4** 57
[39] Ohta Y and Yang J 2014 General rogue waves in the focusing and defocusing Ablowitz–Ladik equations *J. Phys. A: Math. Theor.* **47** 255201
[40] Ohta Y and Yang J 2012 Rogue waves in the Davey–Stewartson I equation *Phys. Rev.* E **86** 036604
[41] Ohta Y and Yang J 2013 Dynamics of rogue waves in the Davey–Stewartson II equation *J. Phys. A: Math. Theor.* **46** 105202
[42] Chen J, Chen Y, Feng B-F, Maruno K-i and Ohta Y 2018 General high-order rogue waves of the (1 + 1)-dimensional Yajima–Oikawa system *J. Phys. Soc. Japan* **87** 094007
[43] Chen J, Chen Y, Feng B-F and Maruno K-i 2015 Rational solutions to two- and one-dimensional multicomponent Yajima–Oikawa systems *Phys. Lett.* A **379** 1510
[44] Chen J, Chen L, Feng B-F and Maruno K-i 2019 High-order rogue waves of a long wave-short model of Newell type *Phys. Rev.* E **100** 052216
[45] Yang B, Chen J and Yang J 2020 Rogue waves in the generalized derivative nonlinear Schrödinger equations *J. Nonlinear Sci.* **30** 3027–56
[46] Yang B and Yang J 2021 General rogue waves in the three-wave resonant interaction systems *IMA J. Appl. Math.* **86** 378–425
[47] Yang B and Yang J 2020 General rogue waves in the Boussinesq equation *J. Phys. Soc. Japan* **89** 024003
[48] Chen S 2013 Twisted rogue-wave pairs in the Sasa–Satsuma equation *Phys. Rev.* E **88** 023202
[49] Akhmediev N, Soto-Crespo J M, Devine N and Hoffmann N P 2015 Rogue wave spectra of the Sasa–Satsuma equation *Physica* D **294** 37–42
[50] Mu G, Qin Z, Grimshaw R and Akhmediev N 2020 Intricate dynamics of rogue waves governed by the Sasa–Satsuma equation *Physica* D **402** 132252
[51] Jimbo M and Miwa T 1983 Solitons and infinite-dimensional Lie algebras *Publ. Res. Inst. Math. Sci.* **19** 943–1001
[52] Wu C F, Wei B, Shi C Y and Feng B-F 2022 Multi-breather solutions to the Sasa–Satsuma equation *Proc. R. Soc.* A **478** 20210711
[53] Ohta Y 2010 Dark soliton solution of Sasa–Satsuma equation *AIP Conf. Proc.* **1212** 114–21
[54] Mu G and Qin Z 2016 Dynamic patterns of high-order rogue waves for Sasa–Satsuma equation *Nonlinear Anal.: Real World Appl.* **31** 179–209
[55] Ling L 2016 The algebraic representation for high order solution of Sasa–Satsuma equation *Discrete Contin. Dyn. Syst.* S **9** 1975
[56] Miyake S, Ohta Y and Satsuma J 1990 A representation of solutions for the KP hierarchy and its algebraic structure *J. Phys. Soc. Japan* **59** 48–55